Preparation of Polystyrene-Encapsulated Silver Nanorods and Nanofibers by Combination of Reverse Micelles, Gas Antisolvent, and Ultrasound Techniques

Jianling Zhang, Zhimin Liu, Buxing Han,* Tao Jiang, Weize Wu, Jing Chen, Zhonghao Li, and Dongxia Liu

Center for Molecular Sciences, Institute of Chemistry, Chinese Academy of Sciences, Beijing 100080, China

Received: August 13, 2003; In Final Form: November 28, 2003

In the present work, we have developed a novel route to synthesize metal nanorods and nanofibers capped by polymer shells, which can be called the reverse micelle–gas antisolvent–ultrasound method. Using this method, we have successfully synthesized Ag core/polystyrene (PS) shell composite nanorods and nanofibers. By changing the ultrasound procedure, PS fibers with discrete embedded Ag particles were formed. The Ag/PS nanocomposites were characterized by transmission electron microscopy (TEM), X-ray diffraction (XRD), UV–vis spectra, X-ray photoelectron spectra (XPS), and FT-IR spectra. The effects of the experimental conditions on the final morphologies of the composite particles were studied. The results show that the length of the composite nanorods is increased with increasing ultrasound time, while the shell thickness depends on the polymer molecular weight.

1. Introduction

Recently, the controlled organization of core–shell particles has aroused intense interest due to its potential use as substrates in surface-enhanced Raman scattering, as heterogeneous and photoelectrochemical catalysts, and as electronic and optical sensors.[1–4] Particularly, polymer-coated particles offer interesting prospects in a broad spectrum in view of their unusual properties.[5–7] The synthetic routes that have been developed in order to produce polymer-coated particles fall into two main classes: polymerization at the particle surface or adsorption onto the particles.[8] The former includes the monomer adsorption onto particles followed by subsequent polymerization,[9] heterocoagulation–polymerization,[10] and emulsion polymerization.[11] The second approach is usually termed the layer-by-layer (LBL) self-assembly technique,[12,13] which allows production of composite materials with tailored compositions and well-defined morphologies such as micro- or nanosized spheres,[14] rods,[15] and wires.[16]

Ultrasound has become an important tool in chemistry in recent years. It has been well-known that ultrasonic radiation in liquids has a variety of physical and chemical effects deriving from acoustic cavitation, which can provide a unique method for driving chemical reactions under extreme conditions.[17,18] Diverse and promising applications of ultrasound have been exploited in material chemistry, such as synthesis of nanostructured materials in various forms,[19–21] preparation of biomaterials,[22,23] and modification for polymers and polymer surfaces.[24–26] Recently, sonochemistry has been extended to produce core–shell type materials. Nanoparticles ZnS[27] or cobalt clusters on silica spheres,[28] alumina core/nickel shell[29] and gold core/palladium shell structured bimetallic nanoparticles,[30] and polyaniline/TiO$_2$ composite particles[31] have been prepared by the ultrasound irradiation.

Carbon dioxide (CO$_2$) is an attractive solvent alternative for a variety of chemical and industrial processes, especially because it is plentiful and inexpensive and has properties that are between those of liquids and gases.[32,33] Currently, there is a great deal of interest in the applications of supercritical (SC) or compressed CO$_2$ in material science.[34] One of the useful techniques in material science is the gas antisolvent process.[35] The principle of this technique is that supercritical (SC) or compressed CO$_2$ is quite soluble in a number of organic solvents and expands them largely. Many solutes are soluble in organic solvents but are not soluble in CO$_2$. Thus the CO$_2$ in organic solvents can act as an antisolvent to precipitate the solutes in the solvent. This technique has been used in different processes, such as extraction and fractionation,[36,37] recrystallization of chemicals,[38] micronization,[39,40] and production of polymeric particles.[41,42] These methods have some potential advantages. For example, it is possible to remove the solvent and antisolvent completely from the products. Moreover, fine particles can be easily obtained because high supersaturation can be achieved in the solution, and the morphologies of the products can be tuned by the pressure of CO$_2$. Recently, we developed a new method to recover the nanoparticles synthesized in reverse micelles using compressed CO$_2$ as antisolvent, and ZnS[43] and Ag[44] nanoparticles synthesized in sodium bis(2-ethylhexyl) sulfosuccinate (AOT) reverse micelles in isooctane were recovered. It was found that, by controlling the pressure of CO$_2$, the ZnS or Ag nanoparticles synthesized in the reverse micelles could be directly precipitated, while the surfactant AOT remains in the solution.

In previous work,[45] we have proposed a method to synthesize Ag nanorods and nanofibers by combination of the reverse micelle and ultrasound techniques. It is interesting to prepare a core–shell composite of which the core metal nanorod or nanowires are capped by polymers, especially when their interaction is not strong. In the present work, we develop a route to synthesize metal nanorods capped by polymer shells, which can be called the reverse micelle–gas antisolvent–ultrasound method. The principle of this method is as following: The inorganic nanoparticles are first synthesized in the reverse micelles in an organic solvent. After the ultrasound treatment for a certain time to induce the formation of silver nanorods,

* To whom correspondence should be addressed. Telephone: 86-10-62562821. Fax: 86-10-62562821. E-mail: Hanbx@iccas.ac.cn.

Polystyrene-Encapsulated Ag Nanorods

J. Phys. Chem. B, Vol. 108, No. 7, 2004 **2201**

the polymer is dissolved in the solution. CO_2 was then added to the solutions to simultaneously precipitate the silver and polystyrene, and meanwhile, the introduction of ultrasound in this process can result in the capping of polymers onto the surfaces of inorganic nanorods. Using this method, we have successfully synthesized Ag core/polystyrene (PS) shell composite nanorods. This method combines four advantages: (1) the Ag nanorods of different lengths can be formed in the reverse micelles induced by ultrasound;[45] (2) compressed CO_2 can force the Ag nanoparticles to come out of the reverse micelles, while the surfactant AOT remains in the solution;[44] (3) the precipitation of polymers from the solution can be controlled by the pressure of CO_2; (4) the presence of ultrasound and CO_2 can result in the beneficial reduction of solution viscosity, which is favorable to the uniform capping of polymers on the surfaces of inorganic nanoparticles.

2. Experimental Section

Material. CO_2 (>99.995% purity) was provided by Beijing Analysis Instrument Factory. The two monodisperse polystyrenes were synthesized by Nanjing Chemical Engineering University, of which the molecular weights were $M_w = 3600$ ($M_w/M_n = 1.06$) and $M_w = 22\,400$ ($M_w/M_n = 1.05$), respectively. The surfactant AOT was purchased from Sigma with a purity of 99%. The solvent cyclohexane (CH) was purchased from Beijing Chemical Factory (>99.5%) and used as received. KBH_4, $AgNO_3$, and ethanol supplied by Beijing Chemical Plant were all AR grade. Double-distilled water was used.

Phase Behavior of Micellar Solution in CO_2. The apparatus for determining the expansion curves and the phase behavior of the reverse micellar solutions was the same as that used to study polymer solutions previously.[46] It consisted mainly of a view cell of 50 mL, a high-pressure pump, a constant temperature water bath, and a pressure gauge. The high-pressure pump was Model DB-80, which was used to charge CO_2 into the system. The accuracy of the pressure gauge, which was composed of a transducer (FOXBORO/ICT) and an indicator, was ±0.025 MPa in the pressure range of 0−20 MPa. The temperature of the water bath was controlled by a HAAKE D8 digital controller, and the accuracy of the temperature measurement was ±0.1 °C.

The reverse micellar solutions were prepared by dissolving the desired amount of AOT and water in cyclohexane ([AOT] = 50 mmol/L; $w = 5$, w stands for the molar ratio of water to AOT). In a typical experiment, 10 mL of reverse micellar solution was charged into the view cell. CO_2 was then charged into the view cell to a suitable pressure after the thermal equilibrium had been reached. A magnetic stirrer was used to enhance the mixing of CO_2 and reverse micellar solution. The volume of the liquid phase did not change with time after equilibrium was reached. The pressure and the volume at equilibrium condition were recorded. More CO_2 was added, and the volume of the liquid phase at another pressure was determined. The volume expansion coefficients were calculated on the basis of the liquid volumes before and after dissolution of CO_2. Some surfactant could be precipitated as the pressure of CO_2 was high enough. The pressure at which the surfactant begins to precipitate is called the cloud point pressure. The cloud point pressure of the solution was also determined.

Precipitation of Silver and PS by UV−Vis Spectra. The procedures to synthesize Ag nanoparticles in the reverse micelles were similar to that reported by other authors.[47] The solution of AOT in cyclohexane was first prepared ([AOT] = 50 mmol/L), and then reverse micellar solutions containing respectively

aqueous solutions of $AgNO_3$ and KBH_4 were prepared by adding corresponding aqueous salt solution to the surfactant solution ($w = 5$). Then the two micellar solutions containing $AgNO_3$ and KBH_4, respectively, were mixed, and silver nanoparticles were formed in the reverse micelles because the water pools can exchange their contents by a collision process.[48]

The precipitation of the silver and polystyrene in compressed CO_2 was determined by the high-pressure UV spectra, of which the temperature-controlled high-pressure sample cell and experimental procedures were the same as those used to study the UV spectra of protein in AOT reverse micelles.[49] In the experiment, the desired amount of PS was dissolved in the reverse micellar solutions containing the synthesized silver nanoparticles under certain temperature. Then the desired amount of solution was added to the high-pressure cell for UV determination. After the thermal equilibrium had been reached, CO_2 was charged into the sample cell by the high-pressure pump until the sample cell was full. For all the experiments at different pressures, the concentration of Ag and PS in the solutions after expansion should be respectively 0.025 and 1.88 mg/mL, if the Ag and PS are not precipitated. The UV spectrum of the solution was recorded by a TU-1201 spectrophotometer every 10 min until it was unchanged, which was an indication of equilibrium condition.

AU: Please note the groups of "X's" in the paragraph below. Please provide the symbol(s) you intended to use here (4 places).

Synthesis of Ag/PS Composite Nanoparticles. The reverse micellar solutions containing respectively aqueous solutions of $AgNO_3$ and KBH_4 were prepared by adding corresponding aqueous salt solution ([$AgNO_3$] = 2[KBH_4] = 0.4 mol/L) to the AOT/cyclohexane solution ([AOT] = 50 mmol/L, $w = 5$). Then the two micellar solutions containing $AgNO_3$ and KBH_4, respectively, were mixed to form silver nanoparticles ([Ag] = 0.2 mg/mL). We carried out the experiments for the synthesis of Ag/PS composites in the two different ways, which are denoted as procedures I and II, respectively. Procedure I is as follows: 35 mL of reverse micellar solutions containing Ag particles was loaded into a sealed flask and treated in the ultrasonic cleaning bath (20 kHz) for a desired time (t_1) to form Ag nanorods in the reverse micelles.[45] Then 65.8 mg of polymer was dissolved in the solution ([PS]$_0$ = 1.88 mg/mL). The mixed solutions were transferred into the cylinder-shaped autoclave of 120 mL, which was treated in the ultrasonic cleaning bath (20 kHz). CO_2 was charged into the autoclave by a high-pressure pump until the desired pressure ($P = 5.50$ MPa) was reached, and the solution was irradiated by ultrasound for the desired time (t_2) to allow the capping of PS with Ag. For procedure II, the desired amount of PS was first dissolved into the reverse micellar solution containing spherical Ag nanoparticles ([AOT] = 50 mmol/L, $w = 5$, [Ag] = 0.2 mg/mL) before ultrasound treatment. Two polymer concentrations of 1.88 and 4.01 mg/mL were studied, respectively. Then 35 mL of solution was loaded into a sealed flask and treated with ultrasound for the desired time ($t_{1'}$), followed by adding antisolvent CO_2 ($P = 5.50$ MPa) and further ultrasound treating for 1 h ($t_{2'}$).

For both of the above two procedures, after releasing solution, the precipitates were collected and washed by water and ethanol several times. The products were dried under vacuum at 303.2 K for 4 h.

Characterization. The morphologies of the obtained particles were determined by transmission electron microscopy (TEM) with a TECNAI 20 PHILIPS electron microscope. Particles were dispersed in ethanol and then directly deposited on the copper grid. X-ray diffraction analysis of the samples was carried out
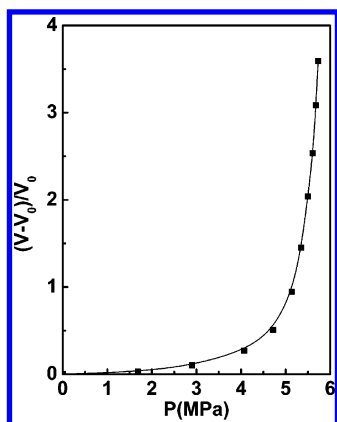
Figure 1. Expansion curve of micellar solution ([AOT] = 50 mmol/L, w = 5) in CO_2 at 301.2 K.

using an X-ray diffractometer (XRD, Model D/MAX2500, Rigaka) with Cu Kα radiation. For UV$-$vis absorption investigation, a certain amount of the obtained Ag/PS powders were dispersed in ethanol and determined by a TU-1201 model spectrophotometer. X-ray photoelectron spectra (XPS) were collected by means of an ESCALab220i-XL spectrometer at a pressure of about 3×10^{-9} mbar using Al Kα as the exciting source ($h\nu$ = 1486.6 eV) and operating at 15 kV and 20 mA. The IR spectrum was recorded using an IR spectrometer (TENSOR 27), and each sample was recorded with 32 scans at an effective resolution of 2 cm^{-1}.

3. Results and Discussion

Volume Expansion and Cloud Point Pressure of Micellar Solution in CO_2. The solution is expended after dissolution of CO_2. Volume expansion coefficient ΔV of the solution at different pressures is a very important parameter for the UV experiments and the coprecipitation process. In this work, ΔV is defined by the following equation.

$$\Delta V = (V - V_0)/V_0 \qquad (1)$$

where V is the volume of the solution saturated with CO_2 and V_0 the volume of the CO_2-free solution. We determined the ΔV of the AOT/water/cyclohexane micellar solution ([AOT] = 50 mmol/L, w = 5) in CO_2 at 301.2 K, which is shown in Figure 1. Evidently, with the increase in pressure, the expansion ratio gradually increases, especially in the high pressure. From the volume expansion, we can know how much solutions should be added to the high-pressure cell in the UV determination and recovery process. The micellar solution becomes cloudy at the cloud point pressure, where the surfactant begins to precipitate. The cloud point pressure of the micellar solutions ([AOT] = 50 mmol/L) determined is 5.58 MPa with a precision of ±0.03 MPa. All of the experiments were conducted at pressures lower than the cloud point pressure for the UV spectrum determination and recovery process, so the precipitation of the surfactant did not occur.

**UV Study on the Coprecipitation of Ag and PS by CO_2.** A key of this method is to precipitate the Ag particles in the reverse micelles and the PS in the solution simultaneously by compressed CO_2 and the AOT remains in the solution. Therefore, we first tested this by UV$-$vis technique. The Ag nanoparticles solubilized in the reverse micelles and the PS dissolved in the solution do not precipitate in the absence of CO_2. As examples, Figure 2 illustrates the UV spectra of the reverse micellar solutions ([AOT] = 50 mmol/L, w = 5) containing the Ag nanoparticles and PS at 301.2 K and some
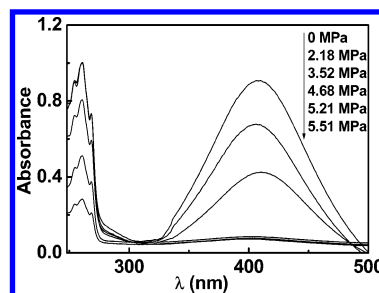
Figure 2. UV spectra of the micellar solution ([AOT] = 50 mmol/L, w = 5) containing Ag and PS at 301.2 K and different CO_2 pressures.
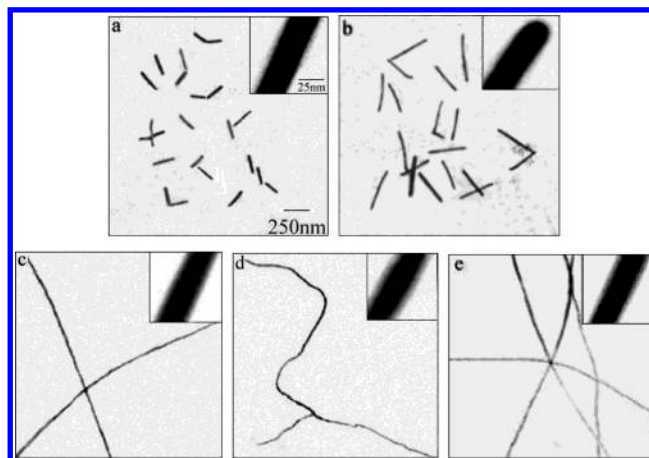
Figure 3. TEM images of Ag/PS composites ([PS]$_0$ = 1.88 mg/mL): (a) t_1 = 0.5 h, t_2 = 1 h, M_w = 3600; (b) t_1 = 1 h, t_2 = 1 h, M_w = 3600; (c) t_1 = 4 h, t_2 = 1 h, M_w = 3600; (d) t_1 = 4 h, t_2 = 1 h, M_w = 22 400; (e) t_1 = 4 h, t_2 = 2 h, M_w = 3600. The insets present the photographs with higher magnification.
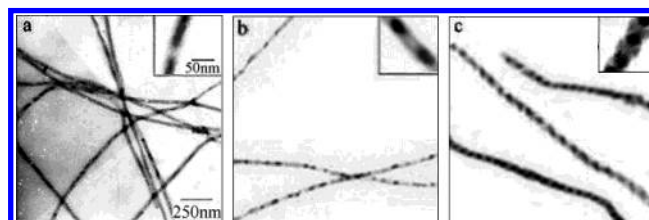

Figure 4. TEM images of Ag/PS composites ($t_{1'}$ = 4 h, $t_{2'}$ = 1 h): (a) M_w = 3600, [PS] = 1.88 mg/mL; (b) M_w = 3600, [PS] = 4.01 mg/mL; (c) M_w = 22 400, [PS] = 4.01 mg/mL. The insets present the photographs with higher magnification.

typical pressures. Evidently, the intensity of the absorption bands for Ag (at about 407 nm) and PS (at about 260 nm) decreases gradually with increasing pressure, indicating the precipitation of Ag and PS. As the pressure reaches 5.51 MPa, which is lower than 5.58 MPa where the surfactant AOT begins to precipitate at this temperature, the absorbance of Ag disappears and that of PS is reduced largely. This illustrates that all of the Ag and most of the PS can be precipitated at this condition, while the surfactant remains in the solution. In other words, the coprecipitation of Ag and PS from the micellar solutions can be realized by controlling the pressure of CO_2.

Morphologies of the Ag/PS Composite Nanoparticles. On the basis of the above studies, we prepared some PS-encapsulated Ag nanorods or nanofibers, which are shown in Figure 3 and Figure 4. The particle size and shell thickness were obtained by measuring all the particles shown in the figures. Figure 3 shows the TEM photographs of the Ag/PS composite nanoparticles obtained by procedure I, and the insets in these figures show the photographs with the larger magnification. As we can see from Figure 3a, after the ultrasound for the micellar

Polystyrene-Encapsulated Ag Nanorods

*J. Phys. Chem. B, Vol. 108, No. 7, 2004* **2203**
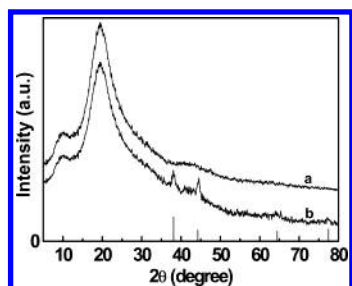
Figure 5. X-ray diffraction patterns of (a) pure PS and (b) Ag/PS nanorods shown in Figure 3c. The vertical lines at the bottom indicate the standard position and relative intensities of fcc silver.

Figure 6. UV−vis spectra of (a) pure Ag nanorod and (b) Ag/PS nanorod shown in Figure 3c.

Figure 7. (a) C 1s and (b) Ag 3d XPS spectra of (1) pure Ag nanorod and (2) Ag/PS nanorod shown in Figure 3c.

solutions of 0.5 h, the silver nanorods encapsulated by polymer shell were obtained, of which the average diameter and shell thickness is about 30 and 5 nm, respectively. By increasing the ultrasound time for the reverse micellar solutions from 0.5 to 1 h, the length of the rod-shaped composite particles increases from 200 ± 40 to 390 ± 30 nm, while the core diameter and shell thickness of the composite rods are nearly unchanged. Given enough time for ultrasonic radiation ($t_1 = 4$ h), the wirelike composites with the length of several micrometers can be obtained (shown in Figure 3c,d). This result is consistent with the previous studies; i.e., with increasing ultrasound time, the length of the pure silver nanorod is increased.[45] From Figure 3c,d, it is found that the shell thickness of the core−shell rods obtained is increased with the increasing molecular weight of the polymer used. The shell thickness does not change considerably with t_2 as t_2 is long enough, as shown in Figure 3d,e, indicating that 1 h is enough for the capping of polymer onto the surface of the silver rods with the aid of ultrasound. The ultrasound used in the antisolvent process played an important role to the capping of polymers on the surface of the Ag nanorods. This was evidenced by the fact that the uncapped mixtures of Ag rods and polymer spherical particles were obtained as $t_2 = 0$.

To further clarify the experimental conditions on the final morphologies of the Ag/PS composite particles, we also synthesized the Ag/PS composites by procedure II, and the TEM photographs are shown in Figure 4. As we can see from Figure 4a,b, the PS fibers (35 ± 5 nm in diameter) with discrete embedded Ag particles are formed, and the core rods encapsulated are shorter at higher PS concentration. In previous work,[45] we have proposed the mechanism for the ultrasound-induced formation of pure inorganic nanorods in reverse micelles, i.e., the reassembly of the micelles caused by ultrasound induces the aggregation of the Ag particles in the reverse micelles. However, the results in Figure 4 show that the Ag particles cannot form longer nanorods in the presence of the PS. The reason may be that the polymer restrains the aggregation of Ag particles because they may be wrapped by the polymer during the ultrasound treatment and the viscosity of solution is larger in the presence of the polymer. This argument is also supported by the results shown in Figure 4c, which was obtained from the solutions with the polymer of higher molecular weight. The polymer nanochains (55 ± 5 nm in diameter) with discrete embedded spherical Ag particles (average size of 30 nm) were formed.

Additional Characterization. The phase structures of the obtained nanorod products were characterized by XRD. As examples, Figure 5 shows the diffraction pattern of the pure PS (curve a) and the composite prepared at 5.50 MPa and 301.2 K (curve b). As shown in the figure, the XRD pattern of the composite shows the broad reflection of the PS and the typical pattern of the face center cubic (fcc) Ag crystalline, of which
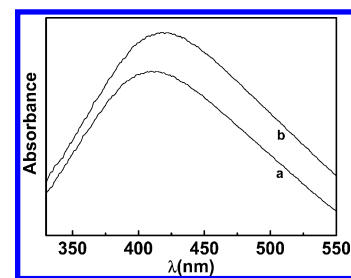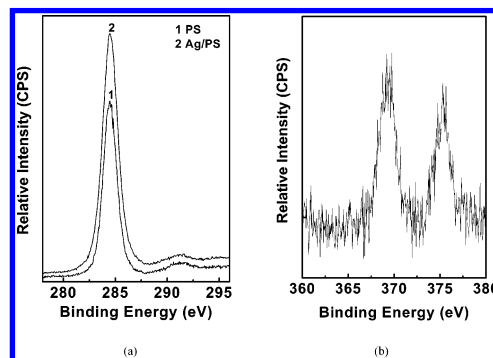
the four diffraction peaks correspond to the 111, 200, 220, and 311 planes (JCPDS File No. 4-0783).

We have characterized the optical properties of the obtained Ag/PS nanorod using UV−visible spectroscopy. Pure polystyrene has no absorption in the wavelength range of around 400 nm. Figure 6 shows the UV−vis absorption spectra of pure Ag nanorod recovered in the absence of PS and the obtained Ag/PS nanorods dispersed in ethanol. Without coating, the pure Ag nanorods in the ethanol solution reveal a plasmon absorption band with maximum (λ_{max}) at 411 nm, while an obvious red-shift can be observed for the PS-coated Ag nanocomposites (λ_{max} = 417 nm). This is due to the higher refractive index of polystyrene than that of ethanol.[50]

The X-ray photoelectron spectra of pure PS and the composites are illustrated in Figure 7. It is evident that the neat PS shows an intense C 1s peak at 284.6 eV. According to the molecular structure of PS, this C 1s peak can be deconvoluted into three distinct components: the aromatic carbon peak at 284.6 eV, the aliphatic carbon peak at 285.0 eV, and the $\pi-\pi^*$ shake-up satellite peak at about 292.0 eV. Figure 7a indicates that the C 1s peak of Ag/PS composites is almost unchanged, which might suggest that there is no strong interaction between Ag and PS matrix. The Ag 3d XPS spectrum of Ag/PS is shown in Figure 7b. The Ag 3d doublet is identified at 369.4 and 375.2 eV for Ag 3d$_{5/2}$ and Ag 3d$_{3/2}$, respectively. The intensity of the Ag 3d photoelectrons was poor due to the shell contributing to the intensity loss. The binding energy (BE) maximum of Ag 3d$_{5/2}$ is higher than that of metallic Ag in the literature (368.3 eV).[51] This may be attributed to the inhomogeneous charging effect caused by the covering of the polymers on the surfaces of the silver rods.

The interfacial interaction between the silver core and the polymer shell was also investigated by FTIR spectra. Parts a and b of Figure 8 show the IR spectra of the pure PS and the PS-capped Ag nanorods, respectively. All the spectra were measured in KBr matrixes. The vibrational bands typical for PS, such as C−H aromatic and aliphatic stretching at 3100 to 2800 cm^{-1} and C═C vibrations at 1492 and 1452 cm^{-1}, are

2204 *J. Phys. Chem. B, Vol. 108, No. 7, 2004*

Zhang et al.
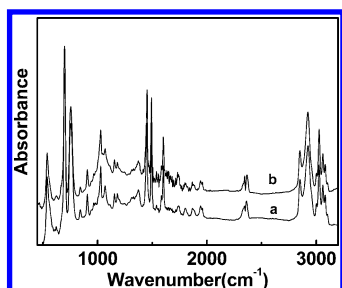
Figure 8. IR spectra of (a) pure PS samples and (b) Ag/PS nanorod shown in Figure 3c.

clearly observed. It was found that the positions of all peaks were identical in both pure PS and Ag/PS. This implies that in the resultant products, there is no chemical linkage or strong interaction between PS and silver nanoparticles, which is consistent with the results of XPS spectra.

4. Conclusion

In summary, this work describes a novel ultrasound-induced method to synthesize the silver/polystyrene composite nanorods from the micellar solutions by antisolvent technique. The size and shell thickness of the composite nanorods can be tuned by the experimental conditions such as the ultrasound time and the molecular weight of the polymer. This process may be easily applied to a range of inorganic/polymer composite nanoparticles with different morphologies, sizes, and shell thicknesses.

References and Notes

(1) Decher, G. *Science* **1997**, *277*, 1232.
(2) Mandal, T. K.; Fleming, M. S.; Walt, D. R. *Nano Lett.* **2002**, *2*, 3.
(3) Gan, D.; Lyon, L. A. *J. Am. Chem. Soc.* **2001**, *123*, 8203.
(4) Lauhon, L. J.; Gudiksen, M. S.; Wang, D.; Lieber, C. M. *Nature* **2002**, *420*, 57.
(5) Marinakos, S. M.; Novak, J. P.; Brousseau, L. C., III; House, A. B.; Edeki, E. M.; Feldhaus, J. C.; Feldheim, D. L. *J. Am. Chem. Soc.* **1999**, *121*, 8518.
(6) Vestal, C. R.; Zhang, Z. J. *J. Am. Chem. Soc.* **2002**, *124*, 14312.
(7) Caruso, F.; Caruso, R. A.; Möhwald, H. *Science* **1998**, *282*, 1111.
(8) Caruso, F. *Adv. Mater.* **2001**, *13*, 11.
(9) Marinakos, S. M.; Shultz, D. A.; Feldheim, D. L. *Adv. Mater.* **1999**, *11*, 34.
(10) Ottewill, R. H.; Schofield, A. B.; Waters, J. A.; Williams, N. S. J. *Colloid Polym. Sci.* **1997**, *275*, 274.
(11) Quaroni, L.; Chumanov, G. *J. Am. Chem. Soc.* **1999**, *121*, 10642.
(12) Caruso, F. *Chem. Eur. J.* **2000**, *6*, 413.
(13) Caruso, F.; Spasova, M.; Saigueirino-Maceira, V.; Liz-Marzán, L. M. *Adv. Mater.* **2001**, *13*, 1090.
(14) Fleming, M. S.; Mandal, T. K.; Walt, D. R. *Chem. Mater.* **2001**, *13*, 2210.
(15) Mayya, K. S.; Gittins, D. I.; Dibaj, A. M.; Caruso, F. *Nano Lett.* **2001**, *1*, 727.

(16) Kovtyukhova, N. I.; Martin, B. R.; Mbindyo, J. K. N.; Smith, P. A.; Razavi, B.; Mayer, T. S.; Mallouk, T. E. *J. Phys. Chem. B* **2001**, *105*, 8762.
(17) Suslick, K. S.; Price, G. J. *Annu. Rev. Mater. Sci.* **1999**, *29*, 295.
(18) Peters, D. *J. Mater. Chem.* **1996**, *6*, 1605.
(19) Cintas, P.; Luche, J. L. *Green Chem.* **1999**, *1*, 115.
(20) Palchik, O.; Kataby, G.; Mastai, Y.; Gedanken, A. *Adv. Mater.* **1999**, *11*, 1289.
(21) Shafi, K. V. P. M.; Ulman, A.; Dyal, A.; Yan, X. Z.; Yang, N. L.; Estournes, C.; Fournes, L.; Wattiaux, A.; White, H.; Rafailovich, M. *Chem. Mater.* **2002**, *14*, 1778.
(22) Langer, R. *Acc. Chem. Res.* **2000**, *33*, 94.
(23) Johnson, L. L.; Peterson, R. V.; Pitt, W. G. *J. Biomater. Sci., Polym. Ed.* **1998**, *9*, 1177.
(24) Hiorns, R. C.; Khoukh, A.; Ghigo, P.; Prim, S.; Francois, J. *Polymer* **2002**, *43*, 3365.
(25) Kim, H.; Lee, J. W. *Polymer* **2002**, *43*, 2585.
(26) Liao, Y. Q.; Wang, Q.; Xia, H. S.; Xu, X.; Baxter, S. M.; Slone, R. V.; Wu, S. G.; Swift, G.; Westmoreland, D. G. *J. Polym. Sci., Part A: Polym. Chem.* **2001**, *39*, 3356.
(27) Arul Dhas, N.; Zaban, A.; Gedanken, A. *Chem. Mater.* **1999**, *11*, 806.
(28) Ramesh, S.; Cohen, Y.; Prosorov, R.; Shafi, K. V. P. M.; Aurbach, D.; Gedanken, A. *J. Phys. Chem. B* **1998**, *102*, 10234.
(29) Zhong, Z.; Mastai, Y.; Koltypin, Y.; Zhao, Y.; Gedanken, A. *Chem. Mater.* **1999**, *11*, 2350.
(30) Mizukoshi, Y.; Fujimoto, T.; Nagata, Y.; Oshima, R.; Maeda, Y. *J. Phys. Chem. B* **2000**, *104*, 6028.
(31) Xia, H.; Wang, Q. *Chem. Mater.* **2002**, *14*, 2158.
(32) Kaiser, J. *Science* **1996**, *274*, 2013.
(33) DeSimone, J. M. *Science* **2002**, *297*, 799.
(34) Cooper, A. I. *Adv. Mater.* **2001**, *13*, 1111.
(35) Reveerchon, E. *J. Supercrit. Fluids* **1999**, *15*, 1.
(36) Winters, M. A.; Frankel, D. Z.; Debenedetti, P. G.; Carey, J.; Devaney, M.; Przybycien, T. M. *Biotechnol. Bioeng.* **1999**, *62*, 247.
(37) Favari, F.; Bertucco, A.; Elvassore, N.; Fermeglia, M. *Chem. Eng. Sci.* **2000**, *55*, 2379.
(38) Muller, M.; Meier, U.; Kessler, A.; Mazzotti, M. *Ind. Eng. Chem. Res.* **2000**, *39*, 2260.
(39) Chattopadhyay, P.; Gupta, R. B. *Ind. Eng. Chem. Res.* **2000**, *39*, 2281.
(40) Sarkari, M.; Darrat, I.; Knutson, B. L. *AIChE J.* **2000**, *46*, 1850.
(41) Li, D.; Liu, Z. M.; Yang, G. Y.; Han, B. X.; Yan, H. K. *Polymer* **2000**, *41*, 5707.
(42) Dixon, D. J.; Lunabarcenas, G.; Johnston, K. P. *Polymer* **1994**, *35*, 3998.
(43) Zhang, J. L.; Han, B. X.; Liu, J. C.; Zhang, X. G.; He, J.; Liu, Z. M. *Chem. Commun.* **2001**, 2724.
(44) Zhang, J. L.; Han, B. X.; Liu, J. C.; Zhang, X. G.; He, J.; Liu, Z. M.; Jiang, T.; Yang, G. Y. *Chem. Eur. J.* **2002**, *8*, 3879.
(45) Zhang, J. L.; Han, B. X.; Liu, M. H.; Liu, D. X.; Dong, Z. X.; Liu, J.; Li, D.; Wang, J.; Dong, B. Z.; Zhao, H.; Rong, L. X. *J. Phys. Chem. B* **2003**, *107*, 3679.
(46) Li, D.; Han, B. X.; Liu, Z. M.; Liu, J.; Zhang, X. G.; Wang, S. G.; Zhang, X. F.; Wang, J.; Dong, B. Z. *Macromolecules* **2001**, *34*, 2195.
(47) Barnickel, P.; Wokaun, A.; Sager, W.; Eicke, H. F. *J. Colloid Interface Sci.* **1992**, *148*, 80.
(48) Fletcher, P. D. I.; Howe, A. M.; Robinson, B. H. *J. Chem. Soc., Faraday Trans. 1* **1987**, *83*, 985.
(49) Zhang, H. F.; Han, B. X.; Yang, G. Y.; Yan, H. K. *J. Colloid Interface Sci.* **2000**, *232*, 269.
(50) Mayya, K. S.; Schoeler, B.; Caruso, F. *Adv. Funct. Mater.* **2003**, *13*, 183.
(51) Moulder, J. F.; Stickle, W. F.; Sobol, P. E.; Bomben, K. D. In *Handbook of X-ray Photoelectron Spectroscopy*; Chastain, J., Ed.; Perkin-Elmer Corporation: Eden Prairie, MN, 1992; p 120.